A precise measurement of the total width of the η' meson

E. Czerwiński[a], D. Grzonka[b], P. Moskal[a,b] for the COSY-11 Collaboration
[a] *Institute of Physics, Jagellonian University, Kraków, Poland*
[b] *Institut für Kernphysik, Forschungszentrum-Jülich, Germany*

Abstract

The physics of the η' meson will receive an increasing relevance in view of the forthcoming measurements planned e.g. at the COSY, DAϕNE-2 and MAMI-C facilities where the η' will be produced in $hadron - hadron$, $e^+ - e^-$, and $\gamma - hadron$ reactions, respectively [1, 2].

Experimentally the emphasis will be put on the studies of the η' meson decays which are of interest on its own and certainly will provide inputs to the phenomenology of the Quantum Chromo-Dynamics in the non-perturbative regime.

Specifically, precise determinations of the partial widths for the η' decay channels will be helpful for the development of the Chiral Perturbation Theory. However, the experimental precision of the partial width for various decay channels – where only the branching ratio is known or will be measured – is governed by the precision of the knowledge of the total width ($\Gamma_{\eta'}$). Therefore, the precise determination of $\Gamma_{\eta'}$ will have a strong impact on the physics results which will be derived from future measurements at the detectors WASA-at-COSY and KLOE.

The width of the η' was established in only two direct measurements with the relative precision of 30% [3] and 50% [4]. The average from these measurements amounts to 0.30 $\pm$ 0.09 MeV and differs from the value of 0.202 $\pm$ 0.016 MeV determined indirectly from the combinations of partial widths obtained from integrated cross sections and branching ratios [5].

The significantly more precise direct determination of the $\Gamma_{\eta'}$ should resolve this discrepancy.

Among previous experiments the one performed by the NIMROD collaboration extracted the width of the η' meson with the smallest error ($\Gamma_{\eta'} = 0.28 \pm 0.1$ MeV) [3]. **At the COSY–11 facility – combined with the excellent features of the COSY proton beam – the ($\Gamma_{\eta'}$) can be determined with at least five times better precision, which will be due to i) an about three times better experimental resolution, ii) an about three times larger statistics, iii) an about four times better signal to background ratio, and finally due to a simultaneous use of two independent methods for the derivation of the width of the η' meson.**

The experience gathered at COSY–11 during the years of operation will allow us to control the systematical errors by two and in the case of some parameters even by three independent methods which details are described in the text.

1 Inroduction

In the last issue of the Review of Particle Physics only two direct measurements of the natural width of the η' meson are reported [5]. In the first experiment the width was established

from the missing mass spectrum of the $\pi^- p \to nX$ reaction measured close to the threshold for the production of the η' meson [3]. The experimental mass resolution achieved was equal to 0.75 MeV/c^2(FWHM) and the extracted value of $\Gamma_{\eta'}$ amounts to 0.28 $\pm$ 0.10 MeV/c^2. In the second experiment the value of $\Gamma_{\eta'}$ was derived from the threshold excitation function of the $pd \to {}^3HeX$ reaction [4]. The study was performed at 20 different beam momenta, however, the error of the $\Gamma_{\eta'}$ was larger than in the previous measurement due to the large relative monitoring uncertainities. In this experiment $\Gamma_{\eta'} = 0.40 \pm 0.22$ MeV/c^2 was determined.
At the COSY–11 facility we intend to combine both techniques and establish the $\Gamma_{\eta'}$ with the precision of 0.02 MeV. We can determine the threshold excitation function for the $pp \to pp\eta'$ reaction and simultaneously we can construct missing mass spectra at various excess energies with an experimental precision of about 0.3 MeV/c^2 (FWHM).

We plan to perform the measurement very close to the kinamatical threshold. The advantage of a study close to the threshold is that the experimental uncertainities for the measurement of ejectiles are much reduced since $\partial(\mathrm{mm})/\partial \mathrm{p}$ tends to zero. Here by mm we denoted the missing mass and by p the momentum of the outgoing proton.

2 Experimental technique

We intend to determine the natural width of the η' meson from the distributions of the missing mass of the $pp \to ppX$ reaction and from the close to threshold excitation function of the total cross section for the $pp \to pp\eta'$ process. We plan to conduct the measurements at four beam momenta close to the kinematical threshold for the $pp \to pp\eta'$ reaction.

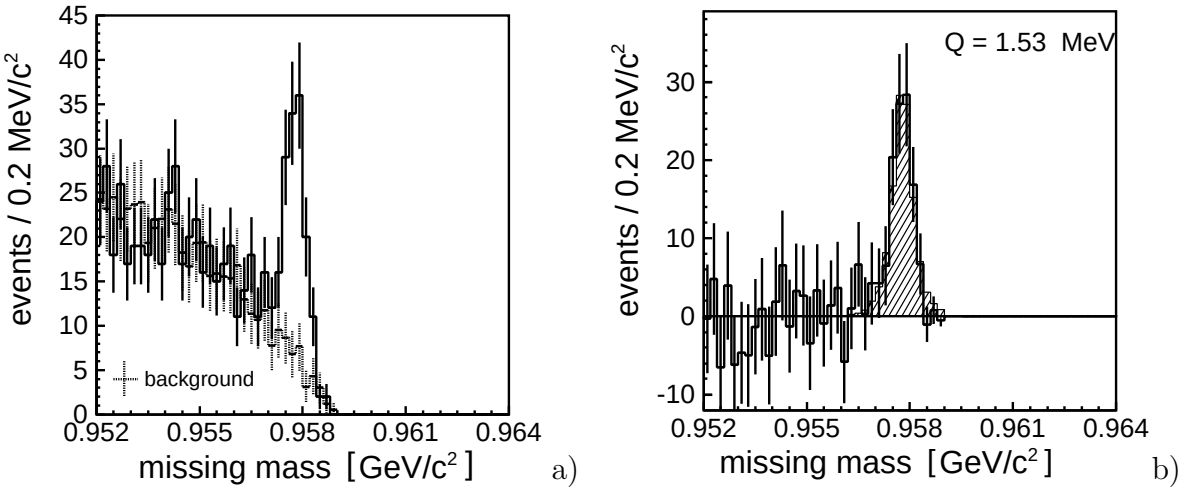

Figure 1: Missing mass distribution with respect to the proton–proton system measured at Q = 1.53 MeV above the threshold of the $pp \to pp\eta'$ reaction [10] (a) before, and (b) after the subtraction of the background. Background shown as dotted lines is combined from the measurements at different energies shifted to the appropriate kinematical limits and normalized to the solid-line histogram. Dashed histograms are obtained by means of the Monte–Carlo simulations.

An example of the missing mass distribution obtained in the previous measurements performed using the COSY-11 setup [11] is presented in figure 1. The form of the spectrum results from the convolution of the experimental resolution and the natural distribution of the mass of the studied meson. Thus, a precise extraction of the total width of the meson demands an iden-

tification of all possible sources of the experimental uncertainities and the reliable estimation of their influence on the measured mass. In the following we will present a thorough investigations aiming in estimation of these effects in the case of the measurements by means of the COSY-11 facility. In our case the mass of an unobserved particle is determined from the momenta of the colliding and outgoing protons. The four-momentum conservation applied to the $pp \rightarrow ppX$ reaction leads to the following expression:

$$m_x^2 = E_x^2 - \vec{P}_x^2 = (E_{beam} + E_{target} - E_1^p - E_2^p)^2 - |\vec{P}_{beam} + \vec{P}_{target} - \vec{P}_1^p - \vec{P}_2^p|^2, \qquad (1)$$

where the used notation is self-explanatory. The momentum of the target protons is by more than 10^6 times smaller than the momenta of the beam and ejectiles and thus can be safely neglected in view of the beam momentum smearing which is on the level of 10^{-4}. Thus clearly the significant contribution to the experimental uncertainities in the determination of the missing mass will originate from the spread of the beam momentum and from the resolution of the determination of the momenta of outgoing protons. We will argue below that both sources of errors are well under control. To raise the confidence of their estimation we will establish their values by at least two independed methods.

2.1 Monitoring of the beam momentum spread

Method 1: Frequency spectrum

The beam momentum smearing can be determined from the measured Schottky frequency spectra and the known beam optics. The Schottky frequency spectrum constitutes a standard monitoring tool at COSY and since many years it is routinely utilised by the COSY-11 group. An example of such a momentum distribution calculated by this method is presented in figure 2. The solid vertical lines indicate a range of the spectrum which is seen by the target with a diameter of 9 mm. When using a target with a width of 1 mm the range of the beam momentum seen by the target will be equal only to 0.2 MeV/c as it is presented by the dashed lines. In the case of the proposed studies we will prepare an aperture for a cluster beam which is 1 mm in the direction perpendicular to the beam and 10 mm along the beam line.

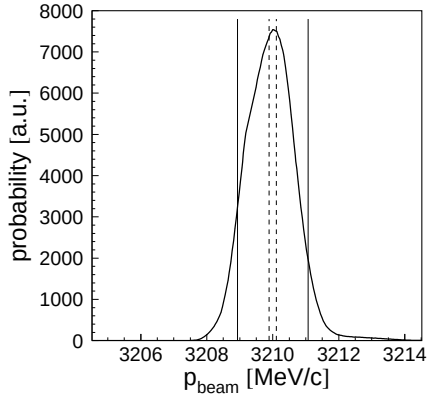

Figure 2: Beam momentum distribution calculated from the Schotky frequency spectrum measured during the COSY-11 run in 2004. The dashed and solid lines showe limits deduced from the target dimensions of 1 mm and 9 mm, respectively, and the very well know dispersion of the COSY beam at the position of the COSY-11 target [6].

Method 2: Narrowing of the missing mass spectrum with decreasing beam momentum

The smearing of the missing mass due to the natural width of the η' remains unaltered when the beam momentum changes. In contrast, the smearing of the missing mass distribution caused by the beam momentum spread will narrow with the decreasing beam momentum and at threshold it will reach a constant value directly proportional to the spread of the beam momentum. For

the regular COSY-11 experiments (conducted with a target of 9 mm diameter and a momentum distribution and dispersion as shown in figure 2) the FWHM of the missing mass distribution, caused by the beam spread, equals to approximately 0.5 MeV/c^2. The corresponding simulated spectrum is presented in figure 3a. This together with the smearing of the η' meson mass (see figure 3b) and the smearing of about 0.2 MeV/c^2 due to the unavoidable effects like e.g. multiple scattering in the air, exit window and detector materials (see figure 4a) results in a mass distribution with FWHM of about 0.7 MeV/c^2 as it was indeed observed at the previous COSY-11 experiments. An example is presented in figure 1. The resolution at threshold can be then significantly improved by decreasing the target dimensions in the direction perpendicular to the beam. Therefore, for this measurement we plan to use a target with a width of 1 mm. This will result in a missing mass resolution of about FWHM = 0.2 MeV/c^2 since the smearing due to the beam momentum will amount to 0.05 MeV only (figure 4b).

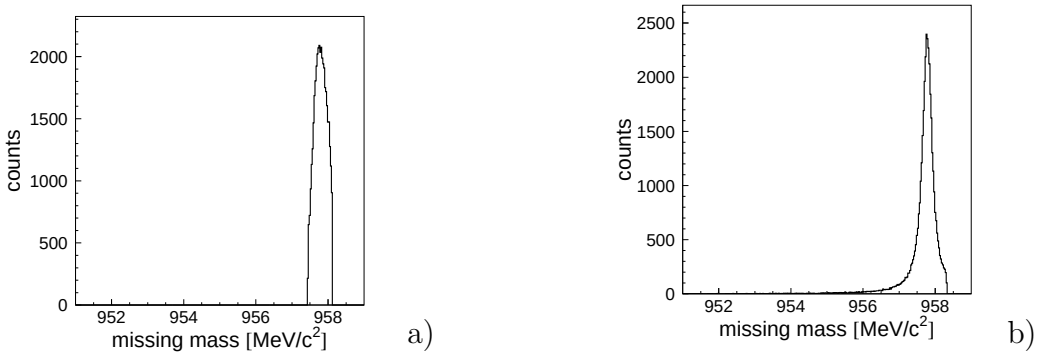

Figure 3: Missing mass spectrum simulated at P_{beam} = 3.210 MeV/c taking into account:
(a) the smearing of the beam momentum cutted by the limits defined from the dispersion and a 9 mm target.
(b) the mass distribution of the η' meson is described by the Breit-Wigner function with a width equal to the mean value obtained from the previous experiments [3, 4] Γ = 0.3 MeV/c^2. In the simulation an ideal detection system with a perfect resolution was assumed.

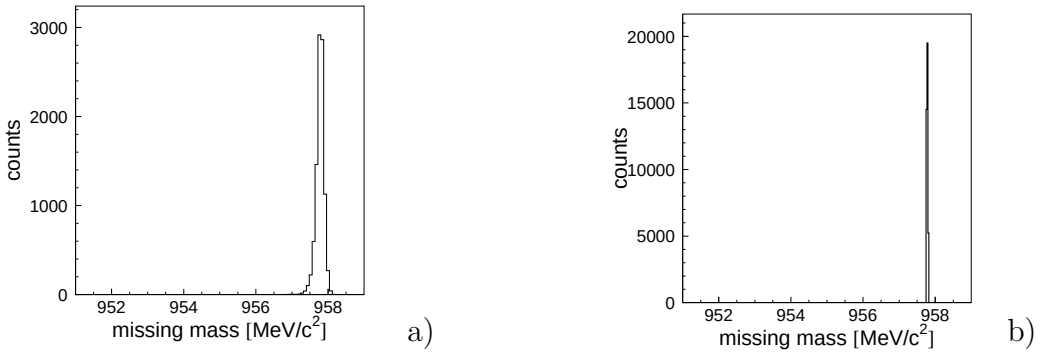

Figure 4: Missing mass spectrum simulated at P_{beam} = 3.210 MeV/c taking into account:
(a) the multiple scattering in the exit window, air and detectors as well as the accuracy of the reconstruction of the ejectiles' trajectories. The latter is burdened also with uncertainities caused by the finite granularity of the map of the magnetic field.
(b) the smearing of the beam momentum cutted by the limits defined from the dispersion and a 1 mm target.

The fact that the missing mass distribution broadens with the increasing beam momentum (with the slope defined by the momentum resolution and the resolution of the determination of the momentum of ejectiles) enables to determine the beam momentum spread by measuring the missing mass spectrum at different beam momenta. The effect for two different spreads of the beam momentum is demonstrated in figure 5. Please note that although the dependence of the shape of the presented dependence from the spread of the beam momentum is not strong the effects from beam momentum spread and the resolution of the momentum determination for the outgoing ejectiles can be separated basing on the angular distribution. This will be demonstrated in subsection 2.2.

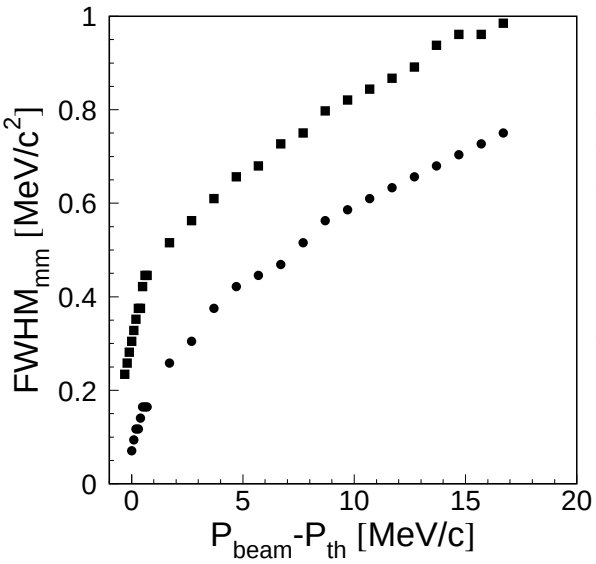

Figure 5: FWHM of the missing mass spectrum as a function of the beam momentum determined assuming that the witdh of the η' meson is equal to zero and that:
(circles)the experimental conditions are as planned for this measurement (target width of 1 mm)
(squares) the experimental conditions are as in the previous runs (target width of 9 mm)

Method 3: Missing mass distribution
In principle the knowledge of the shape of the beam momentum spectrum would also be sufficient provided that it is different from the Breit-Wigner function expected for the mass distribution of the meson η'. Due to the large dispersion, in case of a very narrow target this distribution would be uniform and so would differ significantly from the shape of the Breit-Wigner function. Knowing the shape of the beam momentum distribution its width could be treated as one of the free parameters when comparing the simulated and measured distributions.

2.2 Monitoring of the momentum resolution for registered ejectiles

One of the advantages of a study close to the threshold is that the experimental uncertainities for the measurement of ejectiles are much reduced since $\partial(m_x)/\partial p_{proton}$ tends to zero. However, in a precision experiment they can not be neglected.
In the previous section we mentioned already that the uncertainities of the momentum reconstruction of the registered ejectiles are due to the multiple scattering in the exit window, air, detectors and also due to the finite granularity of the map of the magnetic field. There are still two more effects which are relevant here. Namely, the resolution of the drift chambers and the finite dimension of the interaction region defined by the geometrical beam and target overlap. The latter is important since the reconstruction of the momentum is performed by tracking back the trajectories of the registered particle from the drift chambers to the interaction point which is not known and we assume it to be in the center of the target.

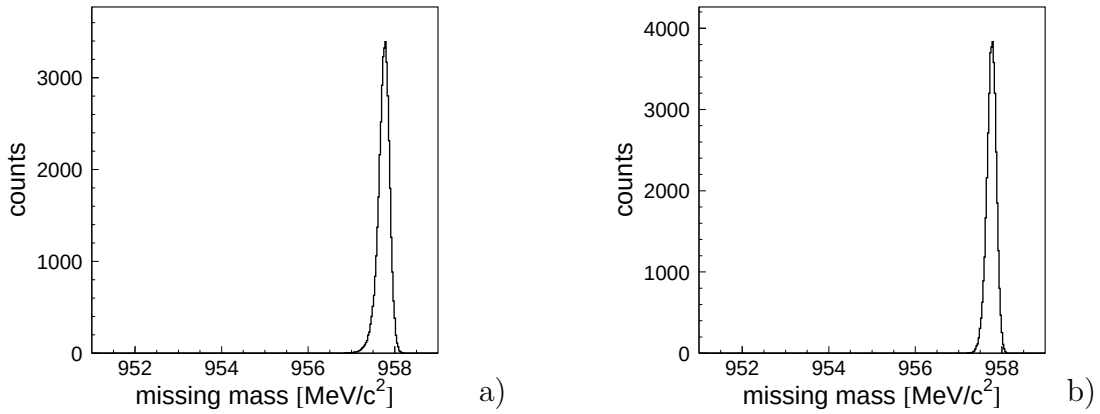

Figure 6: Missing mass spectrum simulated at $P_{beam} = 3.210$ MeV/c taking into account:
(a) the resolution of the momentum reconstruction as it is at present with the 9 mm target and 270 μm of the drift chambers position resolution.
(b) the resolution of the momentum reconstruction as it is expected with 1 mm target and 100 μm of the drift chambers position resolution.

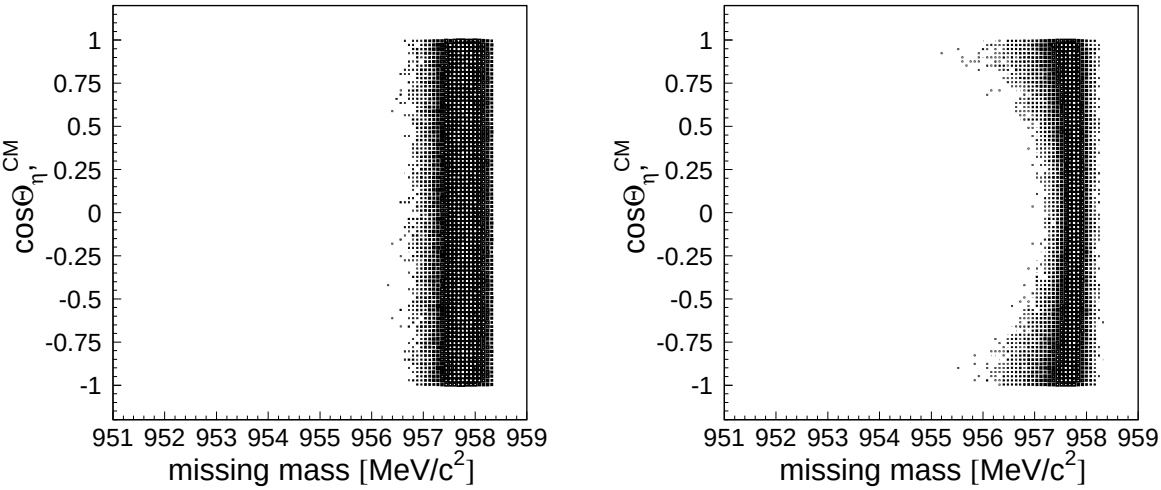

Figure 7: Missing mass distributions of the $pp \to ppX$ reaction simulated for $X = \eta'$ as a function of the cosine of the centre-of-mass polar angle of the emission of the η' meson. The calculations were performed at a beam momentum of 3.210 GeV/c (1.7 MeV/c above the threshold for the η' meson production). (**left**) In the simulation only the smearing of the beam momentum $\sigma_{pb} = 2$ MeV/c was taken into account. (**right**) The beam momentum was fixed to 3.210 GeV/c and only the experimental resolution of the proton momentum reconstruction was considered.

At the previous COSY-11 experiments with the target of 9 mm diameter and the position resolution of a single wire in the drift chamber of 270 μm, the missing mass smearing (due to the uncertainities of the momentum determination of the outgoing protons) was equal to about 0.2 MeV/c^2 as it is shown in figure 6a. Reducing the beam width to 1 mm and simultaneously improving the drift chambers position resolution to 100 μm we expect that this will be reduced by more than 10% (see figure 6b). An improvement of the drift chamber resolution will be achieved by the increase of the voltage on the sence wires from 1600 V to 1900 V. The corresponding

tests have been already performed during the measurement conducted this year in February.

Figure 7 presents simulations performed in order to study the effects on the missing mass uncertainty due to the beam momentum spread and due to the experimental resolution of the momentum determination of the outgoing protons. One sees that the resolution of the missing mass due to the spread of the beam momentum is independent of the polar emission angle of the η' meson, and that the smearing of the missing mass due to the uncertainty of the proton momentum reconstruction does depend on this variable. This example illustrates that from the plot of the polar emission angle of the η' meson versus the missing mass we would be able to distinguish effects originating from the proton momentum reconstruction and from the beam momentum spread.

2.3 Monitoring of the beam and target geometrical parameters

The momentum reconstruction is performed by tracing back trajectories from drift chambers through the dipole magnetic field to the target, which is ideally assumed to be an infinitely thin vertical line. In reality, however, the reactions take place in that region of finite dimensions where beam and target overlap, as depicted in figure 8a. Consequently, assuming in the analysis an infinitesimal target implies a smearing out of the momentum vectors and hence of the resolution of the missing mass signal. Therefore, we have developed a method to monitor this overlap by measuring the elastically scattered protons. The part of the COSY–11 detection setup used for the registration of elastically scattered protons is shown in figure 8b. Trajectories of protons scattered in the forward direction are measured by means of two drift chambers (D1 and D2) and a scintillator hodoscope (S1), whereas the recoil protons are registered in coincidence with the forward ones using a silicon pad detector arrangement (Si) and a scintillation detector (S4). The two–body kinematics gives an unambiguous relation between the scattering angles Θ_1 and Θ_2 of the recoiled and forward flying protons. Therefore, as seen in figure 9a, events of elastically scattered protons can be identified from the correlation line formed between the position in the silicon pad detector Si, and the scintillator hodoscope S1, the latter measured by the two drift chamber stacks. For those protons which are elastically scattered in forward direction and are deflected in the magnetic field of the dipole the momentum vector at the target point can be determined. According to two–body kinematics, momentum components parallel and perpendicular to the beam axis form an ellipse, from which a section is shown as a solid line in figure 9b, superimposed on data selected according to the correlation criterion from figure 9a for elastically scattered events.

In figure 9b, similarly as in figure 9a, it is obvious that data of elastically scattered events arise clearly over a certain low level background. However, what is important here is that the mean of the elastically scattered data is significantly shifted from the expected line, indicating that the reconstructed momenta are on average larger than expected. This discrepancy cannot be explained by an alternative assumption of either the proton beam momentum or the proton beam angle because of the following reason: Trying to reach an acceptable agreement between data and expectation the beam momentum must be changed by more than 120 MeV/c (dashed line in figure 9b), which is almost an order of magnitude more than the estimated error of the absolute beam momentum. Similarly, the effect could have been corrected by changing the beam angle by 40 mrad (see dotted line in figure 9b), which exceeds the admissible deviation of the beam angle ($\pm$ 1 mrad [7]) by at least a factor of 40.

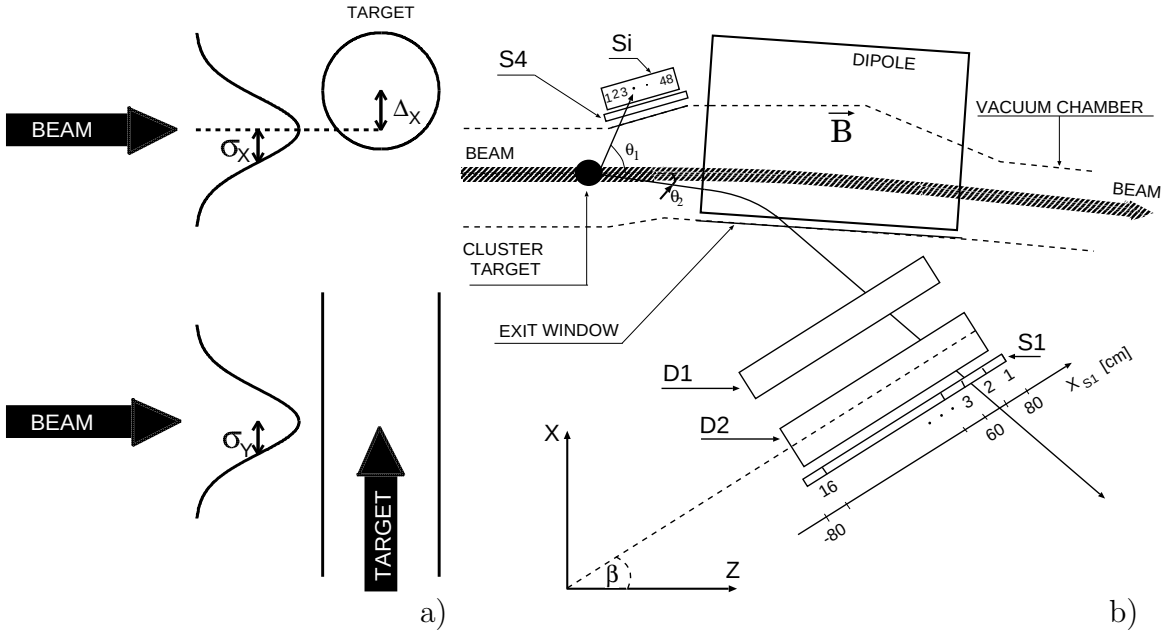

Figure 8: (a) Schematic description of the relative beam and target setting. Seen from above (upper part), and from aside (lower part), σ_X and σ_Y denote the horizontal and vertical standard deviation of the assumed Gaussian distribution of the proton beam density, respectively. The distance between the centres of the proton and the target beam is described as Δ_X.
(b) Schematic view of the COSY–11 detection setup. Only detectors used for the measurement of elastically scattered protons are shown. Numbers, at the silicon pad detector (Si), and below the scintillator hodoscope (S1), indicate the order of segments. D1 and D2 denote drift chambers. The X_{S1} axis is defined such that the first segment of the S1 ends at 80 cm and the sixteenth ends at -80 cm. The proton beam, depicted by a shaded line, circulates in the ring and crosses each time the H_2 cluster target installed in front of one of the bending dipole magnets of the COSY accelerator.

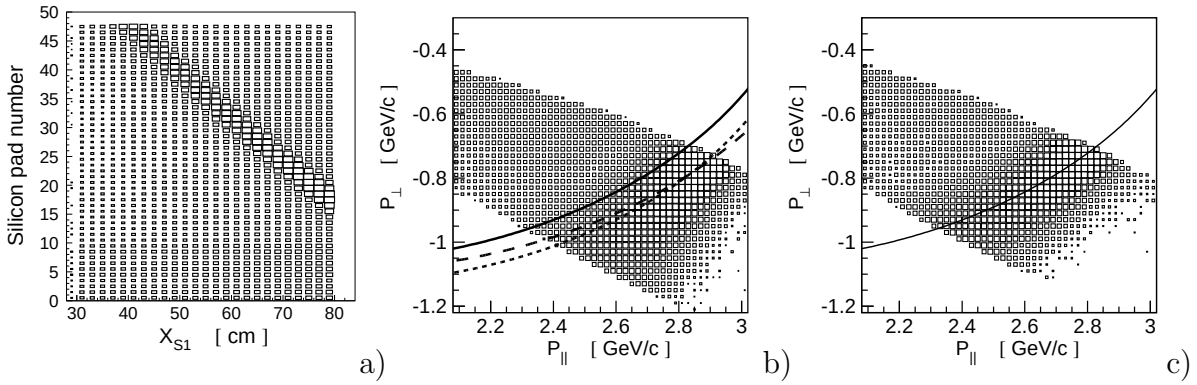

Figure 9: (a) Identification of elastically scattered protons from the correlation of hits in the silicon detector Si and the S1 scintillator hodoscope. Note that the number of entries per bin is given in a logarithmic scale, ranging from 1 (smallest box) to 19000 (largest box).
(b) Perpendicular versus parallel (with respect to the beam direction) momentum components of particles registered at a beam momentum of 3.227 GeV/c. The number of entries per bin is shown logarithmically. The solid line corresponds to the momentum ellipse expected for elastically scattered protons at a beam momentum of 3.227 GeV/c, the dashed line refers to a beam momentum of 3.350 GeV/c, and the dotted line shows the momentum ellipse obtained for a proton beam inclined by 40 mrad.
(c) The same data as shown in b) but analyzed with the target point shifted by -0.2 cm perpendicularly to the beam direction (along the X-axis in figure 8b). The solid line shows the momentum ellipse at a beam momentum of 3.227 GeV/c.

However, the observed discrepancy can be explained by shifting the assumed reaction point relative to the nominal value by -0.2 cm perpendicular to the beam axis towards the center of the COSY–ring along the X-axis defined in figure 8b. The experimentally extracted momentum components obtained under this assumption, shown in figure 9c, agree with the expectation depicted by the solid line, and the data are now spread symmetrically around the ellipse. This spread is essentially due to the finite extensions of the cluster target and the proton beam overlap, which corresponds to about ± 0.2 cm as can easily be inferred from the value of the target shift required.

The above considerations shows that the parallel registration of the elastically scattered protons perimt not only to determine the luminosity but also alows to control the size of the beam and target overlap with the accuracy better than 1 mm. More datails can be found in references [8, 9].

2.4 Signal to background ratio

One of the crucial parameters when deriving the shape of the missing mass spectrum is the relative contribution to the measured signal from the background. In one of the previous measurements [3] the background was as large as the signal and in the other one it was even 10 times larger [4]. In this respect COSY-11 facility offers much better experimental conditions. A signal to background ratio obtained from the previous COSY-11 measurements is presented as points in the below figure (see also figure 1).

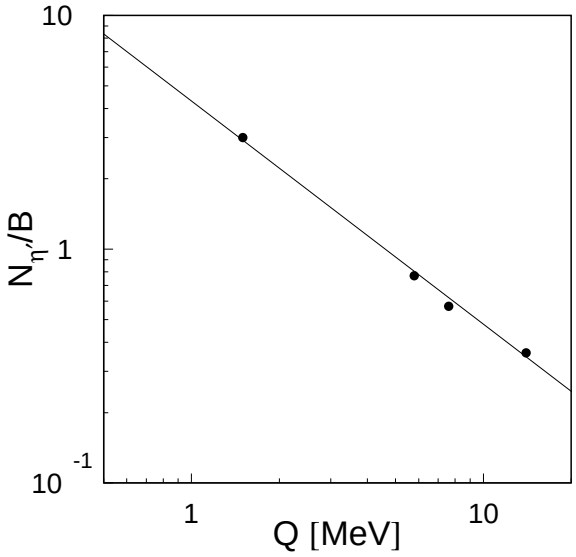

Figure 10: Signal to background ratio obtained for the measurements of the $pp \to pp\eta'$ reaction using the COSY-11 facility. The line is plotted only to guide the eye.

In the excess energy range relevant for this proposal (0.6 MeV $\leq Q \leq$ 2.0 MeV) it varies from 2.2 to 7. However due to the improvement of the experimental resolution which will result from the target reduction to 1 mm, we expect it to be even better. Conservatively we expect the signal to background ratio to vary between 3 and 9.

2.5 Summary of the error estimations

Systematical error

Figure 5(circles) shows that the FWHM of the missing mass spectrum originating from the experimental resolution varies between 0.2 MeV/c^2 and 0.4 MeV/c^2 in the beam momentum range relevant for the discussed experiment (1.5 MeV/c $\leq P_{beam} \leq$ 5.0 MeV/c). Therefore, assuming rather conservatively that we can control this influence with the accuracy of 5% we expect the systematical error in the determination of the missing mass distribution to be lower than $\sigma = 0.01$ MeV/c^2.

Statistical error

In order to estimate the statistical error we have simulated the response of the COSY-11 detection system for the reaction $pp \to pp\eta'$ taking fully into account all experimental conditions and assuming that the width of the η' meson amounts to $\Gamma_{\eta'} = 0.22$ MeV/c^2. Next the generated events were analyzed in the same way as the experimental data and we extracted the plot of the polar emision angle of the η' meson versus the missing mass. In parallel we have created a set of such histograms (high statistics comparison sample) varying the width of the meson η' from 0. to 0.5 MeV. Further on, we have constructed the χ^2 function comparing the test ("experimental") histogram with the histograms from the comparison sample. We have varied freely the magnitude of the histograms from the comparison sample and established the minimum of the χ^2 for each histogram.

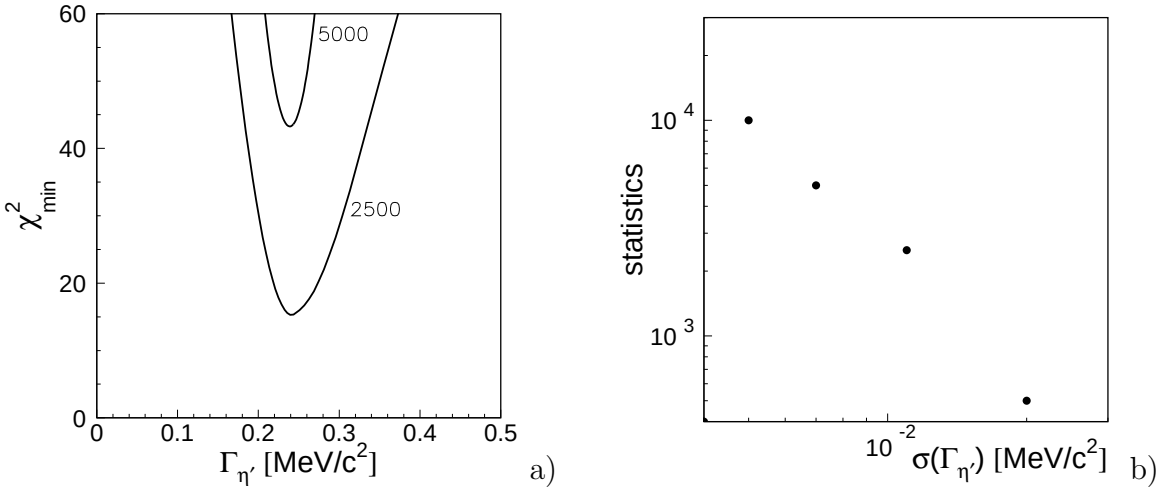

Figure 11: (a) χ^2_{min} as a function of the width of the η' meson.
(b) Expected statistical error for the determination of $\Gamma_{\eta'}$ as a function of the number of reconstructed $pp \to pp\eta'$ events.

In Figure 11a we present an established dependence of the χ^2_{min} as a function of the width of the η'. As expected the miniumum of the obtained distribution is at the value of 0.22 MeV for which a test histogram was created. From the form of the function of χ^2_{min} versus Γ we can deduce the statistical error of the determination of the $\Gamma_{\eta'}$. This will change with the number of registered events and here as an example we present curves obtained in the case when the tested histogram comprised 5000 and 2500 reconstructed $pp \to pp\eta'$ events. Figure 11b shows the dependence of the expected statistical resolution for the $\Gamma_{\eta'}$ determination as a function of the number of the reconstructed events. From the figure one can infer that in order to obtain a statistical error of 0.01 MeV one needs to register and reconstruct about 3000 events.

3 Comparison with the previous experiments

Collaboration Laboratory (year)	$\Gamma_{\eta'}$ $[MeV/c^2]$	Experimental resolution of the missing mass$[MeV/c^2]$	Signal to background ratio	Statistics signal/ background	Observables
NIMROD Rutherford Laboratory (1979)	0.28 ± 0.10	0.75	1	1000/1000	mass distribution
SPES4 SATURNE (1996)	0.40 ± 0.22	–	0.1	4800/48000	threshold excitation function of the cross section
COSY–11 COSY (2006)	? $\pm$ **0.02**	0.3	3–9	2435/627	mass distribution and threshold excitation function and double differential distributions

4 Estimation of the beam time

The aim of the proposed studies is to determine the natural width of the η' meson with an accuracy of ± 0.02 MeV/c^2 This would be five times better than obtained in the previous experiments. According to the estimations discussed in section 2.5 the systematical error of determining the η' meson width will be lower than 0.01 MeV/c^2. In section 2.5 it is also demonstrated that having improved the experimental resolution by the reduction of the target width and by the increase of the drift chamber spatial resolution, we can achieve the same level of the statistial error only if the number of registered and reconstructed $pp \to pp\eta'$ events will be around 3000. With such statistics the overall (sytematical + statistical) error would amount to 0.02 MeV/c^2. Instead of conducting the measurement at a fixed beam momentum we intend to determine the missing mass distributions and the total cross sections for the $pp \to pp\eta'$ reaction at four different beam momenta very close to the kinematical threshold. Measurements at different excess energies will enable us to control the influence of the experimental resolution on the missing

mass and to determine the investigated width from the two independent observables. Namely, from the shape of the missing mass spectrum as well as from the shape of the excitation function of the total cross section. Assuming that the luminosity with a reduced target dimensions will be $2 \cdot 10^{30} cm^{-2} s^{-1}$ and measuring five days for each excess energy listed in the below table we would register in total about 2400 events.

Q $[MeV/c^2]$	Efficiency	Total cross section $\sigma[nb]$	$N_{\eta'}$ number of $pp \to pp\eta'$ events registered per 5 days	B number of background events registered per 5 days	$N_{\eta'}/B$
0.6	0.40	0.77	266	30	9
1.0	0.29	2.04	509	78	6.5
1.5	0.22	3.86	734	188	3.9
2.0	0.18	5.96	926	331	2.9

Basing on the above estimations we ask for **3 weeks** of beam time in the second half of the year 2006.

5 Acknowledgement

We appreciate communication with S. Bass, J. Bijnens, B. Borasoy, P. Hawranek, and F. Kleefeld.

References

[1] H.-H Adam et al, e-Print Archive: nucl-ex/0411038

[2] F. Ambrosino et al., e-Print Archive: hep-ex/0603056

[3] D. M. Binnie *et. al.* Phys. Lett. **B 83** (1979) 141

[4] R. Wurzinger *et. al.* Phys. Lett. **B 374** (1996) 283

[5] S. Eidelman *et. al.* (Particle Data Group), Phys. Lett. **B 592** (2004) 1.

[6] D. Prasuhn, H. Stockhorst, private communication (2006).

[7] D. Prasuhn *et. al.* Nucl. Instr. & Meth. **A 441** (2000) 167.

[8] P. Moskal, e-Print Archive: hep-ph/0408162.

[9] P. Moskal *et. al.* Nucl. Instr. & Meth. **A 466** (2001) 448.

[10] P. Moskal *et. al.* Phys. Lett. **B 474** (2000) 416.

[11] S. Brauksiepe et al., Nucl. Instr. & Meth. **A 376** (1996) 397.